Structural investigation of gaseous, liquid, and solid Br_2 by x-ray absorption

A. Filipponi, L. Ottaviano, M. Passacantando, P. Picozzi, and S. Santucci
Dipartimento di Fisica, Università degli Studi dell' Aquila, Via Vetoio, 67010 Coppito, L'Aquila, Italy
(Received 22 February 1993; revised manuscript received 24 June 1993)

Br K-edge x-ray-absorption measurements have been performed on gaseous (300 K), liquid (294 and 278 K), and solid (200 and 80 K) Br_2. The experimental data have been analyzed by using a comparison with calculated *ab initio* structural signals. The molecular Br–Br average distance, determined with the accuracy of 0.003 Å, shows an expansion of about 0.02 Å going from the gas phase to the low-temperature condensed phases. The bond-distance variance is found to be 2.0×10^{-3} Å^2 in the gas and liquid phases. The intermolecular contribution in the condensed phases, which is found to affect considerably the near-edge region of the spectrum $k < 3.5$ Å^{-1}, has been isolated by means of a subtraction procedure. Significant differences between the liquid samples at the two temperatures are observed and the potential of these measurements to provide information on orientational correlations between neighboring molecules is addressed.

PACS number(s): 61.25.Em, 35.20.Dp, 61.10.Lx, 78.70.Dm

I. INTRODUCTION

The understanding of orientational correlations in liquid halogens represents a major subject of research in the physics of nonelementary liquids. Halogens are among the simplest nonmonatomic liquids which present a nonspherical hard core (the elongation of the molecule increases going from F_2 to I_2) and (at least) quadrupolar interactions. The presence of orientational correlations between neighboring molecules has been unambiguously assessed for the heavy halogens (Cl_2, Br_2, and I_2) and explained in terms of the anisotropy of the intermolecular potential. In a recent review paper [1] many aspects concerning diatomic fluids have been discussed in detail covering theoretical aspects, experiments, and computer simulations.

Experiments on Br_2 have been performed in the gas phase by using spectroscopic techniques [2] and electron diffraction [3,4], in the solid phase (powder) with x-ray [5] and neutron [6] diffraction, and also in the liquid phase by using both x-ray [7,8] and neutron [9,10] diffraction. There is general agreement among the structure factors $S(k)$ of the liquid phase [1], even though some measurements are apparently affected by systematic errors. Reliable atom-atom pair distribution functions [$g(r)$] could be derived and the presence of orientational correlations was confirmed.

Structural information complementary to that provided by the previous techniques can be obtained with the x-ray-absorption spectroscopy (XAS) [11] due to its strong sensitivity to the local structural order. Besides, the presence of coherent multiple-scattering (MS) effects makes the XAS signal sensitive, in principle, to higher order correlation functions in condensed matter [12]. Direct evidence for a three-body structural signal has been found, for instance, in amorphous Si [13] and liquid Ga [14] and Hg [15]. This characteristic makes XAS an extremely promising technique for structural studies of disordered condensed matter.

There has been a large number of XAS investigations dealing with Br_2 in the past 20 years [16–24]. The Br_2 molecule has become a standard for the so called extended x-ray-absorption fine structure (EXAFS) data analysis and the reproduction of its spectrum has been a severe test for the successive refinements of the XAS theory. At the beginning, for instance, it was not possible to reproduce correctly the amplitude of the Br-Br oscillation [16], measured for gas and liquid Br_2 [20], but eventually the inclusion of the photoelectron damping in the model effective potential for the photoelectron made it possible to reach very good agreement in the whole signal [21–23].

Recent investigations show the presence of double-electron excitation effects which modify the smooth behavior of the atomic cross section after the K edge of Br [24]. These effects have been clearly identified in HBr, but exist also in Br_2 and have to be taken into account in any refined structural analysis at the Br K edge.

The subject of the present research deals with an XAS investigation of condensed phases of Br_2. We devoted many experimental efforts to collect reliable and low-noise spectra of Br_2 in the liquid and solid phases as well as of a reference gas sample. The data analysis is performed with the most advanced theory available nowadays, taking full account of the previous experience on the double-electron excitation background problem [24]. A very accurate analysis of the intramolecular contribution in the various phases as well as a reliable extraction of the intermolecular structural signal in the condensed phases will be presented.

The paper is organized as follows. In Sec. II the experimental details concerning sample preparation, data collection, and preliminary reduction are reported. In Sec. III the analysis of the intramolecular contribution is presented, while Sec. IV is devoted to the extraction of the intermolecular contribution in the condensed phases spectra. The conclusions are drawn in Sec. V.

II. EXPERIMENTAL DETAILS

Gaseous, liquid, and solid bromine samples have been prepared using commercial chemical products: Carlo Erba, RPE (Reagente Puro Erba), packed in 1 cm^3 glass ampules.

To obtain accurate and reliable EXAFS amplitudes in Br_2 measurements it is important to avoid any reaction or dissociation of the molecule [20]. This requirement, in conjunction with the limited thickness of windows that can be used for x-ray measurements, generates several experimental difficulties, expecially for the liquid samples. Among the materials which meet the previous requirements we have chosen to use glass containers where possible and 80 μm thick cover glasses as x-ray windows. Different glass portions of the cells were sealed with silicone glue, which does not react with Br_2. It should be noted, however, that a very slow diffusion of Br_2 into this glue occurs in molecular form.

A 16.3 cm long glass cylinder, delimited by composite Mylar (600 μm)/glass (80μm) windows (with the glass on the internal side), sealed with silicone glue, was used for the Br_2 gas measurements. The cell was filled from a side capillary with Br_2 vapors at the vapor pressure of the liquid at 0 °C and then sealed with a flame. The operation temperature of 300(1) K (the uncertainty in the last digit is given in parentheses) guaranteed that no condensation occurred inside the cell and that the density along the optical path remained practically constant during the measurements. The slow diffusion of Br_2 through the glue caused an exponential decay of the internal Br_2 pressure with a time constant of about 2 days. This small effect has been accounted for in the data reduction.

The cell for the liquid Br_2 sample was made of two (80 μm) cover glasses, spaced by about 30 μm, inserted into a longitudinal slot made in a cylindrical glass container (2 cm^3 capacity) acting as a Br_2 reservoir. This flag-shaped cell was sealed with silicone glue. Liquid Br_2, introduced from an aperture of the cylindrical container, filled the thin gap between the cover glasses, generating a uniform layer of liquid suitable for x-ray-absorption measurements. The glass flag-shaped cell was fixed in the center of a sealed polyvinylchloride (PVC) box which was flushed continuously with dry nitrogen at a constant temperature. The box was equipped with Kapton windows for the x-ray-absorption measurements. Measurements of the liquid samples were performed at room temperature 294(2) K and at 278(4) K. In this last case the box was filled with melting ice to make a 0 °C constant temperature bath. The temperature was monitored by means of a chromel-alumel thermocouple attached directly to the glass cylindrical container.

Measurements of crystalline Br_2 were obtained by using two different techniques: the first method was to operate under continuous flow of Ne previously cooled in a liquid nitrogen bath. In this way the Br_2 could be easily cooled to 200(20) K. The second method was to fill the box directly with liquid nitrogen reaching the temperature of 80(−2, +20) K. The coarse temperature control was actually sufficient for the present purpose since structural variations as a function of the temperature, within the same phase, are expected to be rather small. In both cases liquid Br_2 was first solidified with a rapid quench in liquid nitrogen in order to transform the 30 μm liquid layer into a thin layer of randomly oriented Br_2 microcrystals. This requirement, important to obtain measurements free from orientation effects, was only partially achieved.

X-ray absorption measurements have been performed at LURE (Orsay, Paris, France) at the D42-EXAFS I beamline during dedicated beam time. The DCI storage ring was operating at 1.85 GeV with typical currents of 250–300 mA. The beamline is equipped with a channel-cut Si (331) monochromator which allows one to reach the resolution of 10^{-4} at the Br K edge with vertical slits of 1 mm.

Spectra with a typical signal to noise ratio in the 10^4 range were obtained averaging several scans in the energy intervals 13 400–13 650, 13 650–14 000, and 14 000–15 000 eV with energy steps 0.8, 1.5, and 3.0 eV, respectively. For the liquid samples four consecutive scans were recorded in a relatively fast manner (1/2 hour each approximately) to reduce the effects of the instabilities of the sample shape described below.

Some of the measurements were affected by a variation of the effective sample thickness as a function of time. The gas phase data, for instance, have shown an exponential thickness decrease of about 6% during the 3 h of measurement due to the slow diffusion of Br_2 through the silicone glue. Larger thickness fluctuations (up to 30%) occurred in the liquid samples because the glass cell containing liquid Br_2, in equilibrium with its vapor, was extremely sensitive to the temperature. In order to compensate for these unwanted phenomena the spectra have been normalized, prior to averaging, to their actual instantaneous thickness $d(t)$, which was accurately estimated from the absorptance data themselves provided that the thickness variations are slow with respect to the typical spectrum acquisition time. By using this procedure we believe that the thickness variation was compensated and estimate the residual error in the final amplitude of the data of the liquid samples to be below 1%.

The final averaged x-ray-absorption spectra for Br_2 gas 300(2) K, liquid 294(2) K, liquid 278(4) K, solid 200(20) K, and solid 80(−2, +20) K are reported from top to bottom, respectively, in Fig. 1, in the whole energy range. They are labeled for clarity with the symbols g (gas), l (liquid), or s (solid), with the respective temperature in brackets. The near-edge region is reported in Fig. 2 in an expanded range. The K edge of Br_2 is characterized by an evident resonance to the first available "atomic-p-like" molecular state, where the 0 for the energy scale has been placed in Figs. 1 and 2, followed by the onset of the continuum.

The formation of large crystallites or a preferential crystal orientation in the solid phase samples is likely to occur. In this case the spectra are affected by polarization effects, which explain why the amplitude of the edge resonance is not reproducible.

The EXAFS signals extracted by using a conventional three region spline are shown in Fig. 3. The origin of the

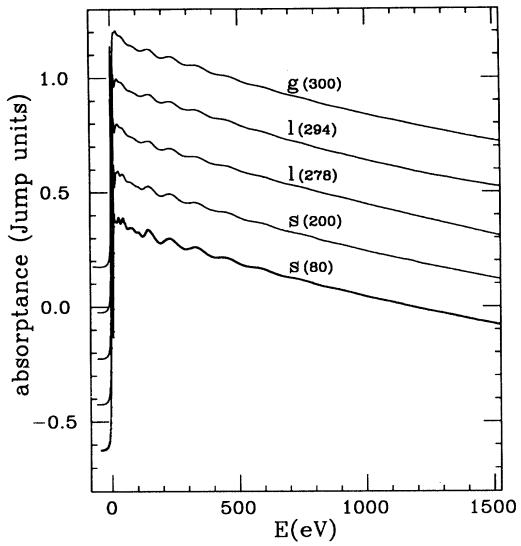

FIG. 1. Raw absorption data as a function of energy. The five curves from top to bottom correspond to Br_2 gas 300(2) K, liquid 294(2) K, liquid 278(4) K, solid 200(20) K, and solid 80(−2, +20) K. The origin of the energy scale is placed on the maximum of the pre-edge resonance peak.

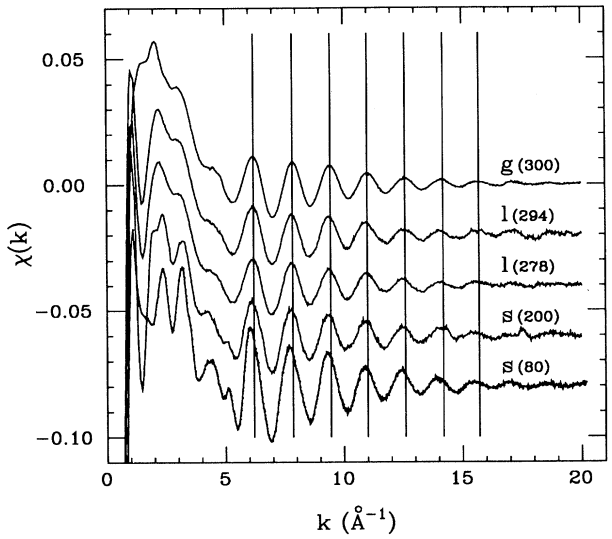

FIG. 3. X-ray absorption fine structure for the various Br_2 samples; the order is the same of that of Fig. 1. The vertical lines correspond to some of the maxima in the gas phase spectrum. The expansion of the Br–Br distance in the condensed phases is evident.

k scale has been conventionally taken in all the spectra to be 6 eV above the maximum of the resonance peak, as indicated with the vertical line in Fig. 2. This represents, at least, a coherent choice among the various spectra. On this scale the EXAFS oscillation associated with the Br–Br distance is evident. The vertical lines drawn in Fig. 3 correspond to the successive maxima of the oscillation in the gas phase spectrum. Notice that the maxima of the other spectra are clearly gradually shifted to lower k values as they were generated by a slightly higher frequency oscillation. This phenomenon is well known and is associated with an average bond-length expansion [11]. In this case, the Br–Br bond average distance appears to increase going from the gas phase to the condensed phases.

Remarkable differences among the various spectra can be seen in Fig. 3 for $k < 6$ Å^{-1}. These features are clearly associated with the appearance of the intermolecular signal in the condensed phases that increases in intensity as the material becomes more ordered.

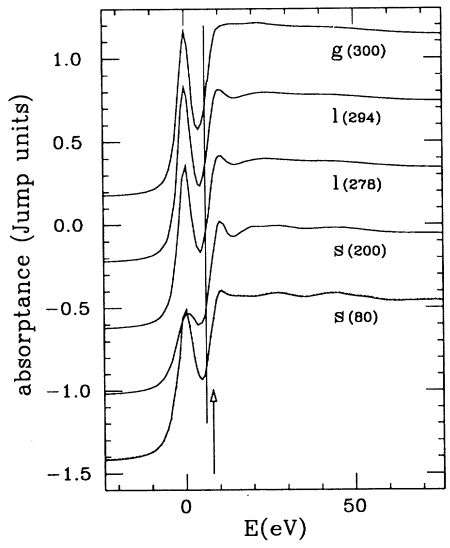

FIG. 2. Br K-edge region for the various Br_2 samples; the order and energy scale is the same of that of Fig. 1. The vertical line at 6 eV indicates the conventional E_0 choice for the k scale, while the vertical arrow at 8 eV indicates the position of the zero of the theoretical energy scale fit to the high energy structural oscillation.

III. DATA ANALYSIS (INTRAMOLECULAR) AND DISCUSSION

The whole set of data has been carefully analyzed in order to extract the structural information associated with both intramolecular and possibly intermolecular contributions.

As a first step we attempted to reproduce the edge region, shown in Fig. 2, with appropriate model functions in order to verify the actual experimental resolution of the monochromator. The spectrum is apparently composed of a single isolated resonance to a bound state followed by the onset of the continuum.

Model functions obtained summing a Lorentzian peak and an arctangent step function were convoluted with a Gaussian (representing the monochromator resolution) and fit to the experimental spectra. The variable parameters were the energy positions of the two contributions, their amplitudes, and the resolution standard deviation δ. Fits of the edges could be obtained with the known value of the core-hole width $\Gamma_{\mathrm{FWHM}} = 2.52$

eV [25] (where FWHM denotes the full width at half maximum) in all cases. The resolution was found to be $\delta = 1.4(2)$ eV.

The edge shape is clearly rather independent of the phase. The energy separation between the resonance and the arctangent inflection point is found to be 6.4(2) eV in the gaseous or liquid cases and practically identical 6.6(2) eV in the solid phase.

Phase shifts have been calculated for the isolated Br_2 molecule up to 120 Ry (ℓ_{max}=24) in the muffin-tin approximation starting from overlapped self-consistent atomic charge densities for the neutral and excited Br atoms. Muffin-tin radii were chosen to be 2.16 a.u., practically tangent at the Br_2 distance of $R_0 = 2.286$ Å adopted for the potential calculation. An energy dependent complex self-energy for the photoelectron effective potential was calculated in the Hedin-Lundqvist approximation [26]. The imaginary part included also a constant factor accounting for the known core-hole width. Br-Br structural signals have been calculated using the GNXAS computer code [27]. The first three terms of the MS series associated with the Br-Br configuration indicated as $\chi_2(k)$, $\chi_4(k)$, and $\chi_6(k)$ have been considered. The calculation provided amplitude $A(k)$, total phase $\psi(k)$, and their first derivatives [$A_1(k)$ and $\psi_1(k)$] with respect to the bond distance calculated at R_0 for each $\chi_n(k)$ term. It appears that the MS series converges quite rapidly in such a diatomic molecular case, and that beyond the main χ_2 signal only the χ_4 term actually needs to be considered. χ_6 and successive signals are quite small and below the noise level of the spectra. This kind of analysis is similar to the one reported in a previous paper [24] for the gas sample. In the present analysis, however, a larger number of angular momenta has been used and the core-hole lifetime has been accounted for directly within the potential.

Fits of the XAFS spectra have been performed using the FITHEO program (GNXAS package). The structural contribution was allowed to vary in phase and amplitude to account for small distance R adjustments and for the thermal variance according to the expression [28]

$$\chi(k) = \mathrm{Im}\left\{ (A + A_1\Delta)\exp[i(\psi + \psi_1\Delta)] \times \left[1 + i\frac{A_1\sigma^2\psi_1}{A}\right]\exp\left[-\frac{1}{2}\psi_1^2\sigma^2\right]\right\}, \quad (1)$$

where $\Delta = R - R_0$ and Im indicates the imaginary part. Notice that in our parametrization R and σ^2 are the mean and variance for the distribution associated with the molecular peaks of the $P(r) = 4\pi\rho r^2 g(r)$ function, which represents the probability density for finding the bonded atom at the distance r.

The K-edge background spectra have been modeled accounting for the contributions from the double-excitation edges $KM_{4,5}$ and $KM_{2,3}$ as previously described [24]. The fit contained initially only three free parameters: the Br–Br bond average distance R, the Br–Br bond distance thermal variance σ^2, and a single nonstructural parameter E_0, representing the energy in the experimental scale corresponding to the zero of the photoelectron theoretical energy scale. Photoelectron damping and core-hole lifetime were previously included in the theory. The effect of the instrumental resolution was accounted for by using the measured value of δ. Successively E_0 has been fixed to the value that appeared to give the most reasonable agreement in all of the five data sets, namely E_0=8 eV above the resonance peak. Notice that this value, indicated as a vertical arrow in Fig. 2, is quite reasonable for the continuum threshold, since it is only about 1.5 eV above the apparent inflection point of the arctangent function fit to the edge. This value is also close to that adopted for the origin of the "experimental" k scale, which makes this conventional choice reasonable. Least squares fits of the experimental spectra have been performed in the range $k \in (4, 20)$ Å^{-1} for the gaseous and liquid (278 K) samples, in the range $k \in (4, 17.5)$ Å^{-1} for the liquid (294 K) sample to exclude some high energy noisy data, and in the range $k \in (9, 20)$ Å^{-1} for the solid samples to exclude the low energy region affected by the intermolecular signal. The experimental and model $k\chi(k)$ signals are reported for comparison in Fig. 4.

The results for the mean value and variance of the intramolecular Br–Br distance are reported in Table I and compared with previous determinations obtained with different techniques. The statistical errors reported in Table I refer to the 95% confidence level. The errors for the bond length R (usually 0.003 Å) do not account for the statistical correlation with the parameter E_0. The correlation between R and E_0 was found to be 0.85 and the correlated errors in R result about twice the reported values. However, the relative alignment of the edges and the common final choice for E_0 has been performed with high accuracy, due the similarity of the spectra, and consequently the uncertainty in E_0 may provide only a sys-

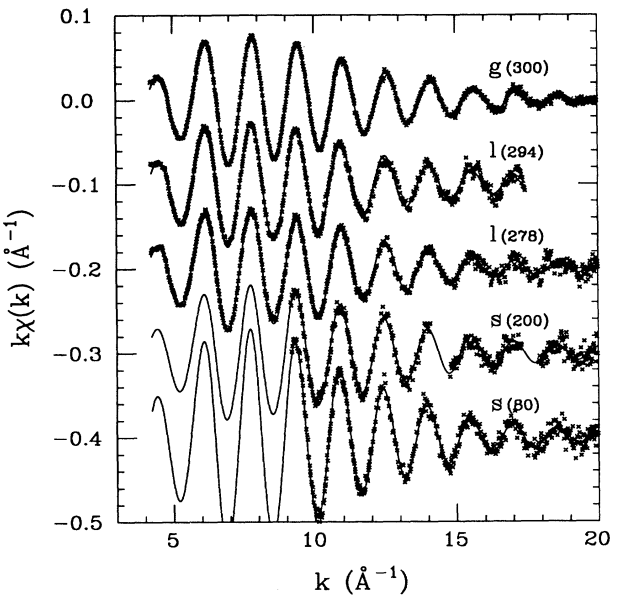

FIG. 4. Model (solid lines) and experimental (crosses) intramolecular Br–Br $k\chi(k)$ signals for the various Br_2 samples. The order is the same of that of Fig. 1.

TABLE I. Average distance R and variance σ^2 for the intramolecular Br–Br bond as a function of the temperature and the phase. The present data are compared with previous determinations based on different methods: (XAS denotes x-ray absorption spectroscopy, Spe denotes spectroscopic, ElD denotes electron diffraction, XRD denotes x-ray diffraction, and ND denotes neutron diffraction).

Phase	Method	T (K)	R (Å)	σ^2 (10^{-3} Å^2)	Ref.
gas	XAS	300(2)	2.288(3)	1.9(2)	this work
liquid	XAS	294(2)	2.302(3)	2.0(3)	this work
liquid	XAS	278(4)	2.302(4)	2.1(4)	this work
solid	XAS	200(20)	2.307(3)	1.4(6)	this work
solid	XAS	80(-2,+20)	2.314(6)		this work
gas	Spe	300	2.2872	2.02	[2,30][a]
gas	ElD	300	2.290	2.0(1)	[3]
gas	ElD	300	2.285		[4]
gas	XAS		2.28		[17]
liquid	XRD	293.0(5)	2.291(2)	2.0(2)	[8]
liquid	ND	298	2.30	3.4	[10]
solid	ND	5	2.301(2)		[6]
solid	ND	80	2.294(2)		[6]
solid	ND	170	2.289(3)		[6]
solid	ND	250	2.286(3)		[6]

[a]Mean value of the $P(r)$ molecular peak estimated accounting for anharmonic effects [30].

tematic error of about ±0.003 Å on the whole set of data.

The very good accuracy in the R parameter is determined by the low noise level and large extension of the data (up to $k = 20$ Å^{-1}), which, comparing the number of oscillations, would correspond to $k = 34$ Å^{-1} in a diffraction experiment.

Our experimental data, reported as a function of the temperature in Fig. 5(a), show unambiguously the expansion of the Br–Br distance passing from the gas phase to the liquid phase and then to the low temperature solid. The increase of the molecular bond length found in the present investigation is very similar to the same one occurring in I_2 [29]. Notice that the XAS technique is really unique in these comparative studies since it allows us to perform equivalent experiments on different condensed phases.

At this level of refinement, the actual meaning of the various distances quoted in the literature requires a more detailed discussion. Our distance determination in the gas phase should be compared with the estimate of the mean value of the $P(r)$ molecular peak, based on spectroscopic data, accounting for anharmonic effects [30]. In this case practically identical values are found. Electron diffraction experiments on gases, as well as x-ray and neutron measurements on the liquids, measure an effective molecular distance fit to the high-k data with the equation

$$S_{\mathrm{mol}}(k) = \frac{\sin kr_a}{kr_a} \exp\left[-\frac{\gamma^2 k^2}{2}\right] , \qquad (2)$$

where r_a and γ^2 are the mean and the variance of the $P(r)/r$ function assumed Gaussian. The mean values of $P(r)$ and $P(r)/r$ do not coincide, but for sufficiently narrow distributions we can write $r_a \sim R(1-(\sigma/R)^2) \neq R$. The difference amounts to about 0.001 Å in our case and can be neglected because it is a factor of at least 3 smaller than the experimental error. Then our results are in extremely good agreement also with electron diffraction determinations in the gas phase and with x-ray or neutron diffraction results in the liquid phase. Notice that due to limited k range available, noise, or systematic errors, the $S(k)$ measurements performed so far [7–10] afford a less precise determination than our XAS data.

There are relatively few diffraction studies of the solid phase [5,6] which, in any case, provide only an indirect measure of the molecular bond distance. Bond lengths, defined as the distances between the average atomic positions, must be corrected for the effect of the librational oscillation of the molecule which reduces the apparent value (foreshortening effect) [31]. The accurate structural determination by Powell, Heal, and Torrie [6] was performed on powder samples and the data were not corrected for this effect, so that their and our results are not immediately comparable. Our two measurements in the crystal phase indeed provide larger bond lengths than their data by approximately 0.8%. This value can very well be the amount of the foreshortening correction in Br_2. On the other hand, the trend of the bond distance as a function of the temperature is extremely similar in the two sets of data.

The bond-distance variance σ^2 can also be measured very accurately with EXAFS because it affects strongly the damping of the oscillation, expecially at high k. The results are reported in Table I and are shown in Fig. 5(b) as a function of the temperature. In the cases of the gaseous and liquid samples the σ^2 parameter has a negligible correlation with the other parameters; for the solid samples instead, because of the amplitude uncertainty due to the possible preferential crystallites orientation, the correlation with the unknown overall intensity makes the determination of σ^2 less accurate. For example, the 80 K data have an apparent Br-Br coordination number of about 1.8, indicating a preferential orientation of the

molecular axis perpendicular to the beam direction. In comparison, the 200 K data are compatible with a Br-Br coordination number of 1 suggesting an acceptable level of disorder in the microcrystallites orientation. For this reason the σ^2 value for the 200 K data appears reliable and is reported in Table I and Fig. 5(b).

The bond-distance variance can be accurately calculated from an Einstein model for the molecular harmonic vibrations in the free molecule and is given by

$$\sigma^2(T) = \frac{\hbar}{2\mu\omega}\coth\left(\frac{\beta\hbar\omega}{2}\right) , \qquad (3)$$

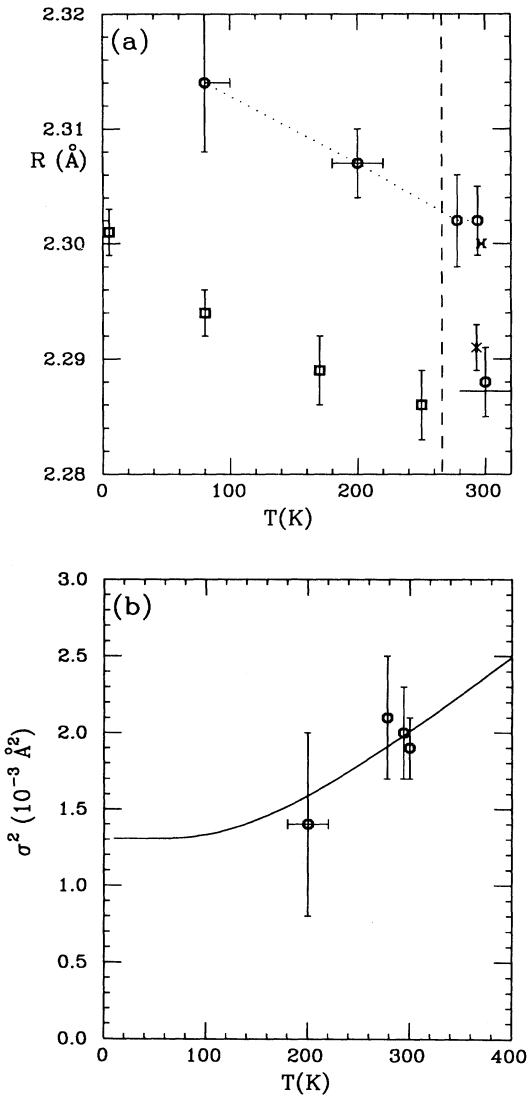

FIG. 5. (a) Molecular Br–Br average bond distance as a function of the temperature: the present data ○ are compared with crystallographic data □, neutron or x-ray diffraction data in the liquid phase × and with the spectroscopic determination (short horizontal line). The freezing point at standard pressure is indicated by the vertical dashed line. (b) Bond distance variance as a function of the temperature. The solid curve corresponds to the Einstein model prediction for $\omega = 323.2$ cm^{-1} [2].

where $\beta = 1/K_BT$, $\omega = 323.2$ cm^{-1} is the molecular stretching frequency [2], and μ is the molecular reduced mass. This estimate, reported as a solid line in Fig. 5(b), yields the value of 2.02(1) 10^{-3} Å^2 at 300 K, which is very close to what is observed by XAFS.

Raman experiments in the solid phase [32] show a series of sharp peaks in the frequency range of 295–300 cm^{-1} corresponding to the stretching modes. The authors are not aware of any infrared or Raman investigation of liquid Br_2; it is likely, however, that similarly to what happens for I_2 [33], the molecular stretching frequency weakens progressively going from the gas to the liquid and then to solid phase, simultaneously to the expansion of the bond length. From these considerations a lowering of the effective Einstein frequency in the condensed phases can be expected which could explain the slight increase in σ^2 from gas to liquid also previously observed [20].

From the previous analysis it appears evident that the XAFS measurements allow one to estimate the molecular structural parameters with a very high accuracy, comparable to or even better than that obtainable with alternative structural techniques. The data indicate unambiguously the progressive expansion of the Br–Br bond length in the condensed phases as the temperature is lowered. These results could be achieved only in the framework of a method for data analysis based on the comparison of the experiment with theoretical signals calculated by using a very refined model for the effective potential "felt" by the photoelectron. In this way several empirical parameters, usually introduced to account for the inelastic damping of the photoelectron, were eliminated.

IV. DATA ANALYSIS (INTERMOLECULAR)

Let us now come to the analysis of the intermolecular contribution in the condensed phases. By visual inspection of Fig. 3 it is clear that the low-k region is strongly affected by the presence of neighboring molecules both in the liquid and in the solid phase. Unfortunately this low-k region is also the one which is largely affected by the anomalies induced by the double-electron excitation edges as demonstrated in the detailed analysis performed on HBr [24]. Due to large sensitivity of multielectron excitation intensities to molecular effects, the HBr background cannot be used to isolate the the structural Br_2 spectrum without introducing systematic errors. Recent theoretical advances in the calculation of double-electron excitation cross sections [34] do not yet produce model spectra with the required accuracy to allow a fully theoretical subtraction of the atomic background, expecially in a molecular case.

A second difficulty consists in the elimination of the intramolecular contribution, which clearly affects also the low-k region. This signal is much more complicated than the corresponding one occurring in diffraction experiments [Eq. (2)] and the limited accuracy of the theory in the near-edge range still prevents us from obtaining an unambiguous extraction of the intermolecular signal free from systematic errors.

After a number of different attempts to analyze the spectra at low-k values the most reliable method to account for the intramolecular and double-electron contributions was to subtract the spectrum of Br_2 gas from those of the liquid samples. Clearly the Br_2 gas spectrum contains all of the background and intramolecular effects that are expected in the spectra of the liquid, and this subtraction procedure is extremely clean from a conceptual point of view. However, it is prone to the introduction of systematic errors and care must be devoted to the choice of the initial data. In the present investigation the raw experimental data have been normalized and scaled by using a careful procedure that generated extremely homogeneous spectra. Due to the very small differences of bond lengths among the various samples the direct subtraction provides already fairly accurate results; however, we used an improved procedure as described in the following paragraph.

Let us write the gas phase and the liquid phase molecular contributions as

$$\chi_g(k) = A(k,R)\ \sin\left[2kR + \phi(k,R)\right]\ , \tag{4a}$$

$$\chi_l(k) = A(k,R+\Delta)\ \sin\left[2k(R+\Delta) + \phi(k,R+\Delta)\right]\ , \tag{4b}$$

respectively. Here Δ represents the difference in the bond lengths. It is clear that the two signals can be obtained with respect to each other with an appropriate scaling of the amplitude and of the k scale. We write Eq. (4b) in terms of Eq. (4a)

$$\chi_l(k) = \chi_g(\tilde{k})\frac{A(k,R+\Delta)}{A(\tilde{k},R)}\ , \tag{5}$$

where $\tilde{k}$ is the solution of the equation: $2\tilde{k}R + \phi(\tilde{k},R) = 2k(R+\Delta) + \phi(k,R+\Delta)$. In practice the k scale is expanded by the factor $\tilde{k} = \frac{R^*+\Delta}{R^*}k$, where $R^* \sim 2.0$ Å is the effective frequency for the Br-Br oscillation. The difference spectra are calculated by using the following equation

$$\chi_{\rm inter}(k) = \chi_l(k) - \chi_g\left(\frac{R^*+\Delta}{R^*}k\right)\frac{A(k,R+\Delta)}{A(\tilde{k},R)}, \tag{6}$$

subtracting from the spectrum of the liquid phase, at each energy point, the spectrum of the gas phase, at a slightly higher energy (to account for the higher frequency in the liquid), scaled by a factor which compensates the wave attenuation. The ratio $A(k,R+\Delta)/A(\tilde{k},R)$ can be calculated easily by using theoretical amplitudes with sufficiently high accuracy. Notice that because of the small Δ/R ratio, amplitudes and phase corrections are rather small and are not a source of additional errors in the final results.

In Fig. 6 we report the results of the subtraction procedure performed on the 294 K data (upper curve), on the 278 K data (middle curve), and on the crystal 200 K data (lower curve). The oscillatory nature of the signals is reliable and represents to a good approximation the intermolecular structural contribution in condensed phases Br_2 XAFS spectra. The two residual signals for the liquid phase are almost identical and, in comparison, resemble a damped version of the 200 K crystal data. The latter spectrum, as previously noted, should correspond to a sufficiently randomized distribution of the crystallites orientations so that the extraction of the intermolecular residual may provide a meaningful comparison with the liquid phase data.

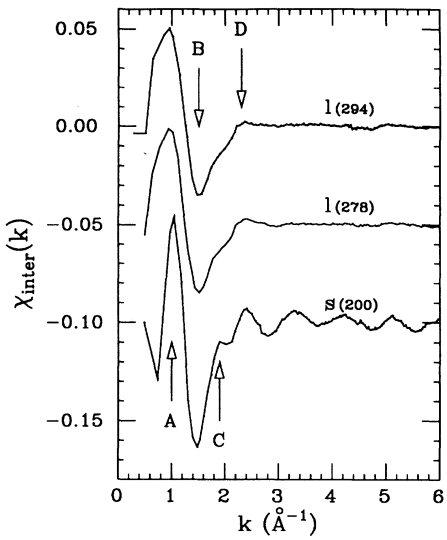

FIG. 6. Intermolecular XAFS signal in condensed phases of Br_2 extracted using the subtraction procedure described in the text. Upper spectrum, liquid 294 K; middle spectrum, liquid 278 K; lower spectrum, crystal 200 K.

All of the residuals (Fig. 6) are characterized by a broad oscillation in the very low-k region with a first maximum (peak A), $\chi = 0.050$ around $k = 1$ Å^{-1}, followed by a minimum B, $\chi = -0.035$ at $k = 1.5$ Å^{-1}, and a successive weaker maximum D, $\chi < 0.01$ at $k = 2.3$ Å^{-1}. Between the minimum B and the maximum D there is an evident shoulder C at $k = 1.9$ Å^{-1}. All of the features A, B, C, and D are clearly visible in either of the three spectra, even though the latter two (C and D) are strongly damped in the liquid-phase residuals. The 200 K residual reveals in addition a clear oscillating behavior extending up to above k=6 Å^{-1} to be associated with the first intermolecular neighbors (two atoms at $\sim$3.35 Å). The liquid phase residuals do not show the evidence for any structural signal above $k \sim 4$ Å^{-1}. Indeed, a certain number of weak features that are systematically present in both spectra were found associated with monochromator glitches and the weak and broad feature around 4–5 Å^{-1} may be due to the incompletely compensated $KM_{4,5}$ edge because of the strong chemical sensitivity of the intensities of double-electron channels.

The differences between the spectra reported in Fig. 6 should be attributed to the effects of the configurational disorder present in the liquid phase which damps out any structural signal above $k \sim 4$ Å^{-1}. This behavior is rather similar to what occurs in the intermolecular $S(k)$ contribution [7–10]. Notice that the features C and

especially D are significantly more intense in the 278 K liquid than in the 294 K liquid, indicating a larger degree of molecular ordering in the cool liquid. This result is not necessarily in contrast with the findings of x-ray and neutron diffraction, which do not show any difference between room temperature and cool liquid, because XAS data and $S(k)$ data are not exactly equivalent. This is an example of how the two techniques probe complementary features of atomic correlations in condensed matter. The fact that the overall shape of the intermolecular signals remains the same upon crystallization may indicate the presence of similar molecular correlations in the two phases. The analysis of the intermolecular signal and of its structural implications requires a large number of multiple scattering calculations of signals associated with several molecular configurations. An analysis of this kind is presently in progress and will be the subject of a successive paper. In spite of its limited extension the intermolecular signal poses structural constraints to the arrangements of the molecules in the liquid phase complementary to those provided by the $S(k)$ data.

V. CONCLUSIONS

The x-ray-absorption spectroscopy was combined with an accurate theory to calculate the structural oscillating contributions to the absorption spectrum of Br_2 and provided values of several molecular parameters. Very accurate determinations of the Br–Br average bond distance in the various phases were made. In this respect XAS has shown to be at least as accurate as electron diffraction or spectroscopic techniques. The Br–Br average distance is shown to increase by about 0.02 Å going from the room temperature gas to the liquid and solid phases. Previous neutron diffraction results are confirmed while a new determination of the Br–Br distance in the solid phase, directly comparable with that of the gas or liquid phases, is obtained.

The intermolecular structural contributions could be isolated by means of a subtraction procedure. The spectrum was dominated by a very large oscillation, of 0.05 units, in the near-edge region which damps out very rapidly vanishing completely above 4 $Å^{-1}$. Significative differences are found between the 294 K and 278 K data in the amplitude of the peak around 2.3 $Å^{-1}$, which should be attributed to the increase in ordering among the neighboring molecules induced by lowering the temperature of the liquid phase.

The overall similarity of the liquid phase intermolecular signals with the crystalline 200 K might have interesting structural implication, possibly indicating the permanence of a similar average local order between the Br_2 molecules. The structural information contained in the intermolecular contributions in the liquid phase, interpreted in the framework of the MS theory and combined with neutron structure factor $S(k)$ data, appears to be helpful in the comprehension of molecular correlation in liquid Br_2 and liquid halogens in general.

ACKNOWLEDGMENTS

Stimulating discussions with C. Andreani and F. P. Ricci are kindly acknowledged. We are indebted to Professor P. Lagarde for his personal support of our research project. Skillful operation of the DCI storage ring by the LURE personnel is acknowledged. Technical support from O. Consorte, W. Galli (Università dell' Aquila), and F. Villain (LURE) is kindly acknowledged.

[1] C. Andreani, J. C. Dore, and F. P. Ricci, Rep. Prog. Phys. **54**, 731 (1991).
[2] G. Herzberg, *Spectra of Diatomic Molecules* (D. Van Nostrand Company, Inc., New York, 1950).
[3] I. L. Karle, J. Chem. Phys. **23**, 1739 (1955).
[4] H. P. Hanson, J. Chem. Phys. **36**, 1043 (1962).
[5] B. Vonnegut and B. E. Warren, J. Am. Chem. Soc. **58**, 2459 (1936); L. L. Hawes, Acta Cryst. **12**, 34 (1959).
[6] B. M. Powell, K. M. Heal, and B. H. Torrie, Mol. Phys. **53**, 929 (1984).
[7] R. W. Gruebel and G. T. Clayton, J. Chem. Phys. **47**, 175 (1967).
[8] A. H. Narten, R. Agrawal, and S. J. Sandler, Mol. Phys. **35**, 1077 (1978).
[9] G. Caglioti and F. P. Ricci, Nuovo Cimento **24**, 103 (1962); P. Ascarelli and G. Caglioti, Nuovo Cimento B **58**, 375 (1966); M. Misawa, Y. Fukushima, K. Suzuki, and S. Takeuchi, Phys. Lett. **45A**, 273 (1973); J. H. Clarke, J. C. Dore, G. Walford, and R. N. Sinclair, Mol. Phys. **31**, 883 (1976); G. W. Stanton, J. H. Clarke, and J. C. Dore, Mol. Phys. **34**, 823 (1977); P. Bisanti and F. Sacchetti, Mol. Phys. **54**, 255 (1985).
[10] C. Andreani, F. Cilloco, L. Nencini, D. Rocca, and R. N. Sinclair, Mol. Phys. **55**, 887 (1985).
[11] P. A. Lee, P. Citrin, P. Eisenberger, and B. Kincaid, Rev. Mod. Phys. **53**, 769 (1981); T. M. Hayes and J. B. Boyce, in *Solid State Physics*, edited by H. Eherenreich, F. Seitz, and D. Turnbull (Academic Press, New York, 1982), Vol. 37, p. 173.
[12] A. Filipponi and A. Di Cicco, Synchrotron Radiat. News **6**, 13 (1993).
[13] A. Filipponi, A. Di Cicco, M. Benfatto, and C. R. Natoli, Europhys. Lett. **13**, 319 (1990).
[14] A. Di Cicco and A. Filipponi, J. Non-Cryst. Solids **156-158**, 102 (1993).
[15] L. Ottaviano, A. Filipponi, A. Di Cicco, S. Santucci, and P. Picozzi, J. Non-Cryst. Solids **156-158**, 112 (1993).
[16] B. M. Kincaid and P. Eisenberger, Phys. Rev. Lett. **34**, 1361 (1975).
[17] P. A. Lee and G. Beni, Phys. Rev. B **15**, 2862 (1977).
[18] E. A. Stern, D. E. Sayers, J. G. Dash, H. Shechter, and B. Bunker, Phys. Rev. Lett. **38**, 767 (1977).
[19] S. M. Heald and E. A. Stern, Phys. Rev. B **17**, 4069 (1978).
[20] E. A. Stern, S. M. Heald, and B. Bunker, Phys. Rev. Lett. **42**, 1372 (1979).
[21] S.-H. Chou, J. J. Rehr, E. A. Stern, and E. R. Davidson, Phys. Rev. B **35**, 2604 (1987).

[22] T. A. Tyson, K. O. Hodgson, C. R. Natoli, and M. Benfatto, Phys. Rev. B **46**, 5997 (1992).
[23] J. Mustre de Leon, J. J. Rehr, S. I. Zabinsky, and R. C. Albers, Phys. Rev. B **44**, 4146 (1991).
[24] P. D' Angelo, A. Di Cicco, A. Filipponi, and N. V. Pavel, Phys. Rev. A **47**, 2055 (1993).
[25] M. O. Krause and J. H. Oliver, J. Phys. Chem. Ref. Data **8**, 329 (1979).
[26] L. Hedin and B. I. Lundqvist, J. Phys. C **4**, 2064 (1971).
[27] A. Filipponi, A. Di Cicco, T. A. Tyson, and C. R. Natoli, Solid State Commun. **78**, 265 (1991).
[28] M. Benfatto, C. R. Natoli, and A. Filipponi, Phys. Rev. B **40**, 9626 (1989).
[29] C. Andreani, M. C. Bellissent-Funel, F. P. Ricci, and M. A. Ricci, Phys. Rev. A **44**, 5018 (1991).
[30] K. Kuchitsu, Bull. Chem. Soc. Jpn. **40**, 498 (1967).
[31] D. W. J. Cruickshank, Acta Cryst. **9**, 757 (1956).
[32] A. Anderson and T. S. Sun, Chem. Phys. Lett. **6**, 611 (1970); G. G. Dumas, F. Vovelle, and J.-P. Viennot, Mol. Phys. **28**, 1345 (1974).
[33] R. J. Magaña and J. S. Lannin, Phys. Rev. B **32**, 3819 (1985).
[34] S. J. Schaphorst, A. F. Kodre, J. Ruscheinski, B. Crasemann, T. Åberg, J. Tulkki, M. H. Chen, Y. Azuma, and G. S. Brown, Phys. Rev. A **47**, 1953 (1993).